High Resolution Imaging with FWI on Wide Azimuth Towed Streamer Data: application in the Mississippi Canyon, GoM

Wanying Wang, Simon Luo, Xiaolei Song, Lennon Infante, Imtiaz Ahmed, Qingsong Li, Ganyuan Xia, Katrina Packer, bp*

Summary

In this study we conducted Full Waveform Inversion (FWI) for an offshore prospect in the Mississippi Canyon protraction area of the GoM to improve the image quality at the reservoir where we observed poor illumination. We used wide azimuth towed streamer (WATS) data with an 11 Hz starting model. We improved model resolution to 24 Hz. The resulting velocity model and FWI derived reflectivity (FDR) reveal previously unseen structures at the reservoir level, and aid interpretation with better horizon continuity throughout the study area as a result of the improved resolution and more consistent image amplitudes.

Introduction

In the Mississippi Canyon area of the Gulf of Mexico, deep sediments with widespread upward migration of salt depositions form pathways for hydrocarbons, but also create great challenges for imaging. Wide shallow salt bodies act as lenses and can cause illumination problems for the regions beneath them (Muerdter and Ratcliff, 2001). The steep dip of the sub-salt target in this area makes it even more challenging when using conventional imaging methods, such as reverse time migration (RTM), which rely on primary reflections. The legacy RTM image for our study area shows a poorly illuminated zone at the boundary of the salt body (Figure 1). The dimmed reflectors beside the dipping salt boundary led to uncertainties during interpretations, and pose significant risks for this prospect. To mitigate the risk, we conducted this study in the hope of extracting more information about the reservoir using existing WATS data.

Since we are limited to the existing data but still seek to improve the image to support interpretation and subsurface characterization efforts, we explore high resolution full waveform inversion (FWI) on the existing WATS data in the area. First introduced by Tarantola (1984), FWI is a data-driven approach that iteratively updates the earth model based on fitting the entire seismic coda. With the development in algorithms and computational power, FWI has gained popularity in velocity model building with proved advantages in resolving complex geological structures (Shen et al, 2017), and capability of reaching the full frequency bandwidth of seismic data (Warner et al, 2021). As high resolution FWI becomes affordable, Zhang et al. (2020) derived reflectivity volume from FWI under the assumption that the inversion can capture fine contrasts in physical properties, and found it provides more balanced illumination compared to RTM results.

In this study, we used an existing 11 Hz FWI velocity model for the initial model (Figure 2a), and ran FWI up to 24 Hz frequency band with processed WATS data. We derived FDR images for each frequency band. The results provide improved image quality throughout the study area, and reduces the illumination gap with more clear salt boundary and horizons at the sub-salt target area, which aids better informed business decision making.

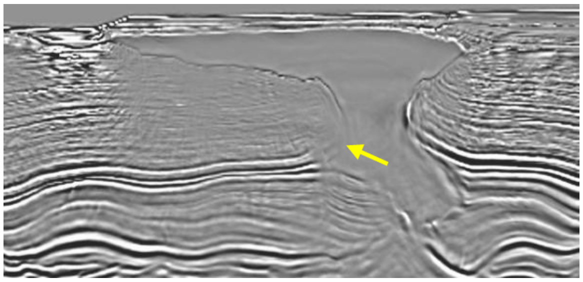

Figure 2: Cross section view of the legacy RTM of the study area. The yellow arrow points to the area with poor illumination.

Data and Method

We used WATS data and an 11 Hz FWI starting velocity model. We created a regional data mask which eliminates the contributions from the receiver locations outside of the starting model area. During the data pre-processing stage, the phase change due to attenuation was corrected through phase-only Q compensation. However, the starting model was built with raw data. We explored the potential of adjusting the source wavelet with a constant time shift, to partially correct for the effect of Q compensation, but the

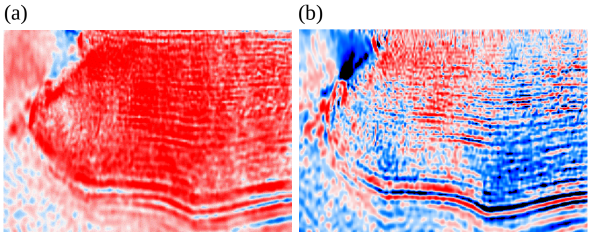

Figure 1: Initial gradient from (a) original data that is pre-processed with phase-only Q compensation, and (b) data after Q compensation is reversed.

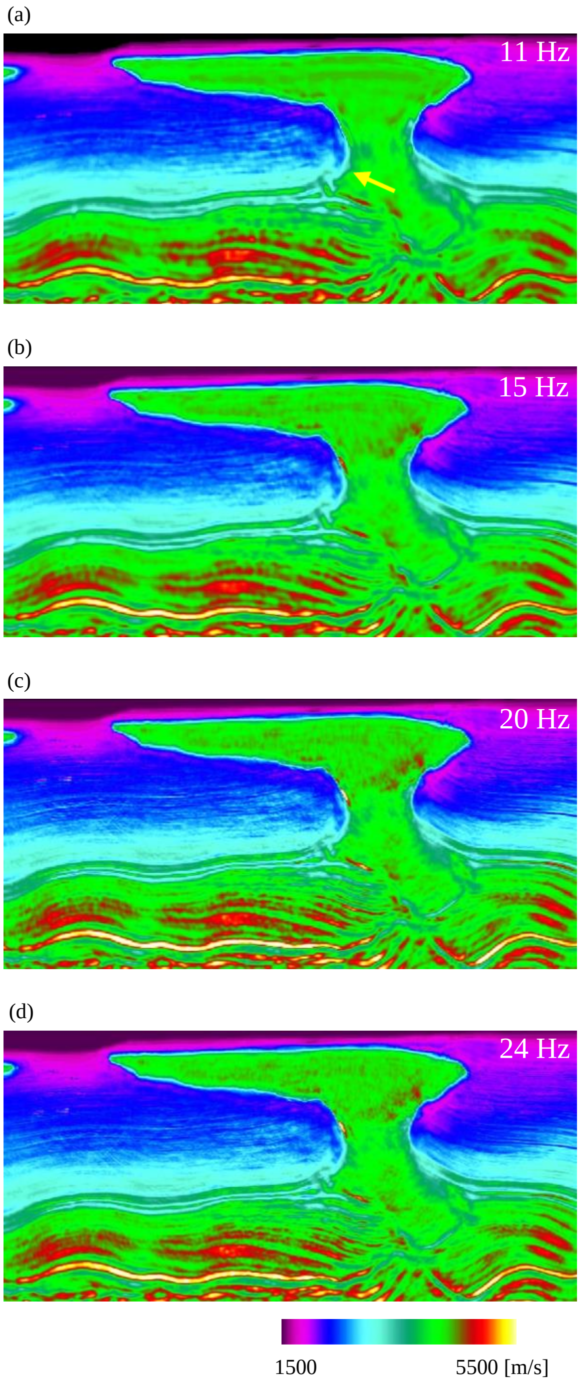

Figure 3: Cross section view of the FWI velocity models, including (a) the 11 Hz starting model, and the results from (b) the 15 Hz frequency band, (c) the 20 Hz frequency band, and (d) the 24 Hz frequency band. The yellow arrow points to the slow velocity patch.

results were not fully satisfactory. In the initial gradient, we see a systematic shift in certain areas (Figure 2a). Though the shift can be corrected through iterations, the overall gradient response lacks distinctive signatures from the geological structures due to the inconsistency in wavefields. We thus applied the reference-time correction method developed by Xia (2005) with a constant Q value to reverse the Q compensation. Using the treated data, the initial gradient shows a more balanced update direction that is closer to zero mean, suggesting both fast and slow velocity updates (Figure 2b).

We first increased the FWI frequency to 15 Hz from the starting model, after which we can see improved imaging on both sides of the salt body with more detailed structures (Figure 3b). We then take this velocity model as input to run the 20 Hz frequency band. Initially, while monitoring the updates in each iteration, we observed slower convergence in this frequency band, due to weaker signal at higher frequency. We increased the contribution of the high frequency content in the data through spectral shaping by applying a filter that enhances the higher frequency band (Figure 4). The resulting velocity model shows significant resolution improvement with the augmented high frequency content (Figure 3c), comparing to the 15 Hz FWI (Figure 3b). We can see the significant resolution boost by comparing the reflectivity images derived from the velocity models using data after spectral shaping to that using non-shaped data (Figure 5a & b). Similarly, we shaped the data and weighted the high frequency content for the 24 Hz

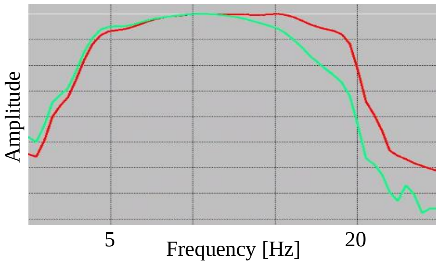

Figure 4: Amplitude spectrums of the 20 Hz frequency band data before spectral shaping (green) and after spectral shaping (red).

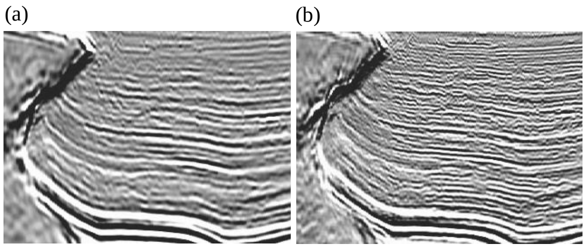

Figure 5: FDRs from the velocity models using the 20 Hz frequency band data (a) before spectral shaping, and (b) after spectral shaping.

frequency band. As shown by Figure 3d, the updated velocity models show further improvement in resolution on both sides of the salt.

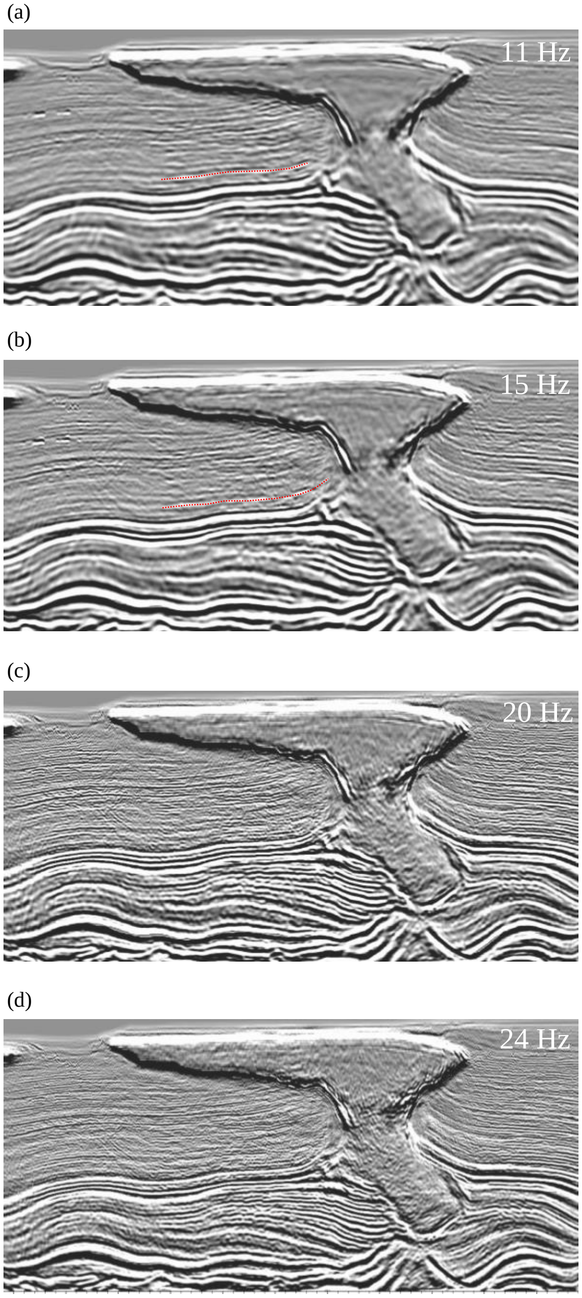

Figure 6: Cross section view of the FDR images derived from (a) the 11 Hz starting model, (b) the 15 Hz velocity model, (c) the 20 Hz velocity model, and (d) the 24 Hz velocity model.

Results

In the starting model, we see a low velocity patch at the edge of the salt, as pointed to by the yellow arrow in Figure 3a. The low velocity patch is gradually corrected in the higher frequency bands (Figure 3b – d). Similar velocity updates can be seen at the right edge of the salt body. With the corrected velocity, the shape of the salt boundary is better defined.

We derived FDR images for each frequency band as shown in Figure 6. In the 11 Hz FDR, which is derived from the starting model, the boundary of the salt is not clearly imaged (Figure 6a). To the left of the salt body, the part of the horizon marked in red is clearly imaged. However, when we trace it towards the salt body, we are not able to identify any continuous patterns. It is thus hard to understand how the horizon and the salt boundary intersect.

As we move to the 15 Hz frequency band (Figure 6b), we start to see the same horizon extend closer to the left edge of the salt body. The boundary of the salt is more clearly defined. We can see the horizons to the left of the boundary show similar dipping angles.

In the 20 Hz FDR as shown in Figure 6c, we see a significant boost in resolution in addition to the improved horizon continuity. The horizons can be more accurately located. In Figure 6d, the 24 Hz FDR shows even higher resolution at the horizons close to the salt boundary and in the deeper part of the image. However, in the higher frequency bands, we also see more cross-cutting noises, so all three bands are being used jointly during interpretation for the best subsurface description.

To the right side of the salt body, we see consistent resolution improvements in the higher frequency bands. This improvement is especially significant when comparing the 20 and 24 Hz FDRs (Figure 6c & d) to the lower frequency ones (Figure 6a & b). The greater details in the horizons provide constraints on the regional structural setting and the intersections at the salt boundary.

We can see the effect from using high resolution images on interpretation more clearly from Figure 7. The yellow dotted line in Figure 7a shows the interpretation based on 11 Hz FDR. When we overlay it with the interpretation for the same horizon based on the 20 Hz FDR (Figure 7b), we see significant differences between the two interpretations as the horizons approach the salt boundary.

Conclusions and Discussion

In this study we demonstrated how we were able to improve the image quality for a Mississippi Canyon prospect using high frequency FWI. We used processed WATS data after reversing the phase-only Q compensation. We started from an 11 Hz velocity model and ran FWI in three frequency bands: 15 Hz, 20 Hz, and 24 Hz. High resolution FWI models show improved illumination at steeply dipping sub-salt reflectors. FDR images generated for each frequency band revealed salt boundary and horizons with better continuity, and improved overall imaging quality with more consistent amplitudes.

In areas where long-offset OBN data are not available and a reasonable low frequency velocity model can be obtained through conventional meanings, FWI application, coupled with conventional model update methods (e.g., salt scenario testing and tomography) can provide significant value. There is wealth of publications on successful applications of FWI on surface towed streamer data (e.g., Vandrasi et al., 2022; Huang et al., 2023; Vigh, 2019). Such applications are often limited to relatively lower frequencies, in particular for large area application. Pushing for higher FWI frequency, such as demonstrated in this study, offers significant value in extracting more information from existing data.

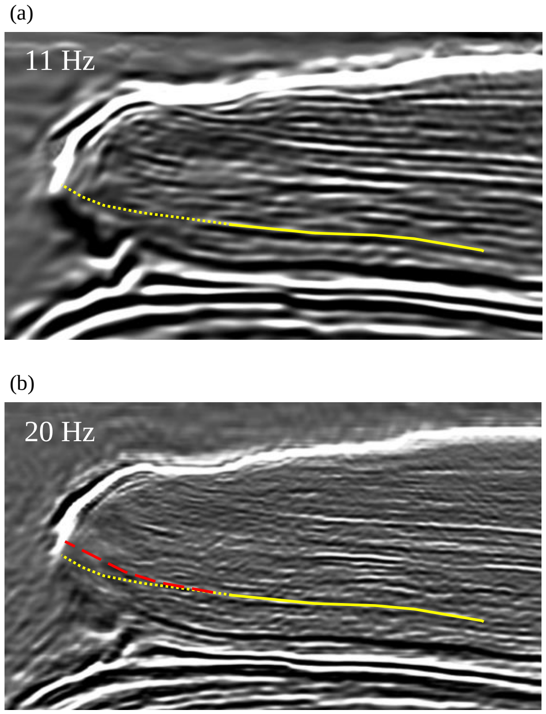

Figure 7: Interpretations based on (a) the 11 Hz FDR, and (b) the 20 Hz FDR. The yellow solid line shows the horizon based on both the 11 Hz and 20 Hz FDRs. The yellow dotted line shows the interpretation based on the 11 Hz FDR. The red dashed line shows the interpretation based on the 20 Hz FDR.

Acknowledgements

We thank bp for permission to publish. This work is done with the support from colleagues at bp Seismic Technology group and Center for High Performance Computing (CHPC). We acknowledge TGS for permission to use the underlying seismic data.